Biology of Reproduction, 2017, 96(3), 531–541
doi:10.1095/biolreprod.116.145367
Research Article
Advance Access Publication Date: 1 March 2017

OXFORD

Research Article

Prosurvival effect of cumulus prostaglandin G/H synthase 2/prostaglandin2 signaling on bovine blastocyst: impact on in vivo posthatching development†

Fabienne Nuttinck[1,*], Alice Jouneau[1], Gilles Charpigny[1], Isabelle Hue[1], Christophe Richard[1], Pierre Adenot[1], Sylvie Ruffini[1], Ludivine Laffont[1], Martine Chebrout[1], Véronique Duranthon[1] and Brigitte Marquant-Le Guienne[2]

[1]UMR BDR, INRA, ENVA, Université Paris Saclay, Jouy en Josas, France and [2]Recherche et Développement, ALLICE, Jouy en Josas, France

*Correspondence: ENVA, Ecole Nationale Vétérinaire d'Alfort, UMR 1198 Biologie du Développement et Reproduction, INRA – ENVA, 7 Avenue du Général DE GAULLE, F-94704 Maisons-Alfort, France. Tel: +33-1-34652008; Fax: +33-1-34652364; E-mail: fabienne.nuttinck@inra.fr

†**Grant Support:** This work was supported by INRA "incentive credits" funding.

Received 29 September 2016; Revised 23 December 2016; Accepted 24 January 2017

Abstract

Apoptotic activity is a common physiological process which culminates at the blastocyst stage in the preimplantation embryo of many mammals. The degree of embryonic cell death can be influenced by the oocyte microenvironment. However, the prognostic significance of the incidence of apoptosis remains undefined. Prostaglandin E2 (PGE2) derived from prostaglandin G/H synthase-2 (PTGS2) activity is a well-known prosurvival factor that is mainly studied in oncology. PGE2 is the predominant PTGS2-derived prostaglandin present in the oocyte microenvironment during the periconceptional period. Using an in vitro model of bovine embryo production followed by transfer and collection procedures, we investigated the impact of periconceptional PGE2 on the occurrence of spontaneous apoptosis in embryos and on subsequent in vivo posthatching development. Different periconceptional PGE2 environments were obtained using NS-398, a specific inhibitor of PTGS2 activity, and exogenous PGE2. We assessed the level of embryonic cell death in blastocysts at day 8 postfertilization by counting total cell numbers, by the immunohistochemical staining of active caspase-3, and by quantifying terminal deoxynucleotidyl transferase-mediated dUTP nick-end labeling signals and apoptosis regulator (BCL-2/BAX) mRNA expression. Morphometric parameters were used to estimate the developmental stage of the embryonic disk and the extent of trophoblast elongation on day 15 conceptuses. Our findings indicate that periconceptional PGE2 signaling durably impacts oocytes, conferring increased resistance to spontaneous apoptosis in blastocysts and promoting embryonic disk development and the elongation process during preimplantation development.

Summary Sentence

PTGS2 activity in expanding cumulus cells and associated PGE2 production promote both the embryonic cell survival of blastocysts and posthatching development at the levels of both the embryonic disk and extra-embryonic tissues in cattle.

Key words: cumulus–oocyte interaction, cyclooxygenase, prostaglandin synthase, lipid mediator, embryo, apoptosis, gastrulation, cell-proliferation.

Introduction

During the early development of eutherian mammals, the fertilized oocyte undergoes cell divisions and cavitation to form a blastocyst [1,2]. When the fluid-filled blastocoel cavity forms, blastomeres segregate between the inner cell mass (ICM) and trophectoderm (TE), which in turn give rise to the first three lineages: the embryonic epiblast, the extraembryonic hypoblast, and the trophoblast [3]. The blastocyst expands and hatches out of the zona pellucida. Like the embryos of most Artiodactyla, hatched bovine blastocysts undergo the elongation process which results from TE development. The morphological transition from ovoid to tubular conceptus occurs concomitantly with the onset of gastrulation. The ICM grows and differentiates to an embryonic disk, through an epithelization step resumed likely by the following sequence: ICM, germ disk, epiblast [4–9]. In cattle, all these events take place before implantation, during the first 2 weeks after fertilization.

Apoptotic activity is a common feature in the preimplantation embryo of many mammals [10–12]. Apoptosis appears spontaneously during the embryonic genome activation (EGA) period and peaks at the blastocyst stage. Embryonic apoptosis is thought to indicate a normal, developmentally controlled, elimination of cells. In cattle, spontaneous apoptosis is observed from the 8–16 cell stage. A wave of embryonic cell death occurs during development of the nonexpanded to the hatched blastocyst, and mainly concerns the ICM [13–16]. The degree of ICM cell death varies considerably between embryos, whether they are produced in vivo or in vitro. Several studies have reported the influence of the environment during early development on the degree of embryo apoptosis [16–20]. Alterations to the oocyte microenvironment, specifically during the periconceptional period, may be reflected by subsequent blastocyst characteristics in terms of blastomere number, caspase-3 activation, DNA fragmentation, and apoptosis-linked gene expression including BCL-2 and BAX, an anti- and a pro-apoptotic member of the BCL-2 family, respectively. The prognostic significance of the incidence of ICM cell death to the developmental potential of the blastocyst remains unclear, mainly due to the lack of studies beyond the blastocyst stage [13,15].

In cattle, the greatest bovine embryo losses occur during the first 2 weeks following fertilization [21,22]. The quality of the preovulatory follicle has been identified as being one of the major reasons for pregnancy losses at the start of pregnancy [22,23]. The developmental potential of the oocyte has been shown to be reflected in cumulus gene expression [24,25]. Higher prostaglandin G/H synthase-2 (PTGS2) expression in the human periconceptional cumulus is correlated with oocytes that develop into higher quality embryos [26]. Prostaglandin E2 (PGE2) is the predominant PTGS2-derived prostaglandin found in the microenvironment of periconceptional oocytes in several mammalian species [27–29]. In response to the gonadotropin surge, the somatic compartment of the preovulatory follicle, and particularly the cumulus cells (CC) that are closely associated with the oocyte to form the cumulus–oocyte complex (COC), produce PGE2, an arachidonic acid-derived lipid mediator. In vivo, the PGE2 concentration in follicular fluid reaches 0.1–1 μM just before ovulation [29]. Follicular PGE2 synthesis results from the sequential action of PTGS2, the inducible PTGS isoform, and specific PGE synthases [30,31]. The cellular effects of PGE2 are mediated through a family of G-protein-coupled receptors designated as PTGER 1 to 4 [32]. In cattle, PTGER2, PTGER3, and PTGER4 are expressed in CC, whereas PTGER2 is the only PGE2 receptor subtype expressed in the oocyte [33]. Cumulus PTGS2 expression and associated PGE2 production are critical for successful cumulus expansion and oocyte maturation processes [34]. Previous in vitro studies performed in our laboratory had shown that the PGE2 produced by CCs enhances mitogen-activated protein kinase activity in maturing oocytes and promotes meiosis progression in cattle [33]. As well as its role in the terminal differentiation of the COC, the PTGS2/PGE2 pathway affects preimplantation embryonic development. We have previously shown that the pharmacological inhibition of PTGS2 activity achieved by exposing COCs to 8 μM NS-398 during the in vitro maturation/fertilization (IVM/IVF) period slowed down the cell cycle kinetic throughout in vitro development (IVD) and produced embryos with reduced numbers of cells at the time of blastocoelic cavity formation [33]. The involvement of PTGS2-related PGE2 was shown to restore normal IVD through 1 μM PGE2 supplementation during NS-398-treated IVM and IVF.

Numerous studies in cancer research have reported that the upregulation of PTGS2 expression and associated PGE2 production exert direct anti-apoptotic effects through PTGER2 [35,36]. While the role of PTGS2-derived PGE2 in promoting cancer cell survival is acknowledged, its involvement in the regulation of physiological apoptosis during early development remains so far unexplored. In the present work, we investigated whether PGE2 present in the oocyte microenvironment during the periconceptional period impacted (i) spontaneous apoptotic activity occurring at the blastocyste stage and (ii) subsequent posthatching development, which has been undetermined so far. We used our well-established in vitro model of maturation (IVM), fertilization (IVF), and embryonic development (IVD) in cattle to investigate the effects of different periconceptional PGE2 environments on embryonic cell death. The MIV/FIV culture media were supplemented with NS-398, a specific inhibitor of PTGS2 activity, and/or with exogenous PGE2. Embryo apoptosis was assessed by counting total blastomere numbers, analyzing extensive oligonucleosomal DNA fragmentation using terminal deoxynucleotidyl transferase-mediated dUTP nick-end labeling (TUNEL) and active caspase-3 localization, and finally by quantifying the gene expression ratio for apoptosis regulator (BCL-2/BAX). In addition, after transfer to recipient uteri and collection at day 15 of pregnancy, as previously reported [37–39], the in vivo posthatching development of blastocysts produced differentially in vitro was evaluated using morphometric analyses.

Materials and methods

Animals

Animals were managed in accordance with the European Community Directive 2010/63/UE and under the license of the French

Table 1. Primer pairs used for real-time qRT-PCR.

Gene	Accession no.	Sequence	Product size (bp)	Reference
BCL2	NM_001166486	5′-TCGTGGCCTTCTTTGAGTTC-3′ 5′-CGGTTCAGGTACTCGGTCAT-3′	109	[44]
BAX	NM_173894.1	5′-CTCCCCGAGAGGTCTTTTTC-3′ 5′-TCGAAGGAAGTCCAATGTCC-3′	176	[44]

Institute of Agricultural Research (INRA-UCEA). The experiments were performed at the same National Institute of Agricultural Research (INRA) experimental farm (registered under N°FRTB910 in the national registry for experimental farms) for various experimental protocols. The staff in charge of animal treatments and embryo collection possessed the regulatory level 1 and level 2 authorizations from the French veterinary services. All protocols were approved by the local Animal Care and Use Committee and, for the later collection periods, by the local Ethics Committee (Registered as N_12/070 in the National Ethics Committee registry). The authorizations allowing in vitro embryo production and embryo transfer were granted by the French Veterinary Services (N°FRPB780, FRBP940, and 91–536). All recipients (n = 28) were Holstein heifers (age, 1.62 ± 0.13 years). The animals were housed in the same building and fed the same diet (grass silage, hay, straw, concentrates). Their average growth was 0.360 kg ± 0.260 per day over the experimental period, with a body condition score ranging from 2.75 to 3.25 on a 1 to 5 scale [40]. Oestrus was detected regularly and recorded five times daily by experienced herdsmen. All the animals used were cycling before the start of the protocol.

Embryo production

Bovine ovaries were collected at the slaughterhouse, and COCs were aspirated from 3 to 6 mm antral follicles. Only oocytes surrounded by more than three compact layers of CCs were selected. Following three washes in HEPES-buffered M199 (Sigma), groups of up to 50 immature COCs were transferred to four-well plates (Nunc, Roskilde, Denmark) containing 500 μl of a defined maturation medium consisting of TCM199 (Sigma, Saint-Quentin Fallavier, France) supplemented with 10 ng/ml epidermal growth factor (mouse EGF, Sigma) and 4 mg/ml bovine serum albumin (BSA) at 38.5°C in a water-saturated atmosphere under 5% carbon dioxide. After a 22 h culture period, the COCs underwent IVF as previously described [41]. Depending on the experiment and as previously described [33], 8 μM NS-398 (Cayman Chemicals), a selective PTGS2 inhibitor, used alone or supplemented with 1 μM PGE2 (Cayman Chemicals), or 0.1, 1, 10 μM PGE2 alone, was added to the maturation and fertilization medium. NS-398 and PGE2 were dissolved in DMSO (D-4540, Sigma). Stock solutions of NS-398 (8 mM) and PGE2 (0.1, 1, 10 mM) were prepared and stored at –20°C until use. On the day of the experiment, each stock solution was further diluted by 1:1000 in the culture medium to reach the desired concentrations. The final concentration of DMSO (0.5%, v/v) in the culture medium was the same in all treatment groups. An additional group, containing the same volume of DMSO only, was included in each experiment as a control. After IVF, presumptive zygotes were denuded and transferred into 50 μl droplets (under paraffin oil) of modified synthetic oviduct fluid [42] supplemented with 6 mg/ml BSA and 10 mM glycin. The embryos were cultured for 7 or 8 days at 38.5°C in a water-saturated atmosphere under 5% CO_2/5% O_2/90% N_2. The rate of blastocyst development was determined at the end of culture. The day of fertilization was considered as day 0. At day 1 postfertilization (1 dpf), noncleaved (single-cell) oocytes were separated from those that had cleaved. At 4 dpf, the embryos were transferred into fresh medium. For the embryonic apoptosis experiment, embryos were harvested after 8 days of DIV culture, corresponding to the wave of spontaneous ICM cell death. The 8 dpf embryos collected were either stored at –80°C until RT-PCR analysis or fixed for 1 h at 4°C in 2.5% (w/v) paraformaldehyde (Sigma) in PBS, transferred to PBS, and stored at 4°C until the TUNEL assay and active caspase-3 immunohistochemistry. For the posthatching development experiment, embryos recovered after 7 days of DIV culture were graded on the basis of their morphological appearance, according to the Manual of the International Embryo Transfer Society. Only grade-I day 7 postfertilization blastocysts and expanded blastocysts were selected for transfer. The embryos were transferred nonsurgically to the uterine horn ipsilateral to the corpus luteum of previously synchronized recipients, 7 days after oestrus and according to the protocol previously described [38]. Seven to ten embryos were transferred to each recipient animal. Four recipient animals, one per IVM/IVF treatment (control, 8 μM NS-398 alone, 8 μM NS-398+ 1 μM PGE2, 1 μM PGE2 alone), were used for each embryo transfer session. These embryo transfer sessions were repeated in order to collect a minimum of 10 to 15 day 15 embryos per IVM/IVF treatment. Each heifer was used only once to minimize the impact of the maternal environment on posthatching development data. The collection of day 15 embryos was performed transcervically according to the protocol used routinely in our laboratory [37]. Each day 15 conceptus recovered was characterized morphologically under a stereomicroscope in terms of total length and embryonic disk/epiblast features (presence or absence, round, elliptic, long axis parallel or not to the elongation axis of the conceptus). The length of conceptuses was only recorded for those with intact ends. Each embryonic disk was photographed under a stereomicroscope coupled to an Axiocam ICC1 camera (Zeiss) and its area was assessed using the open-source software ImageJ (http://rsbweb.nih.gov/ij/).

Analysis of BCL-2/BAX expression in 8 dpf embryos using real-time qRT-PCR

Reverse transcription and real-time PCR quantifications were performed as previously described [33]. For each IVM/IVF treatment, three pools of ten 8 dpf embryos were analyzed. Briefly, total RNA was extracted using the PicoPure RNA isolation kit (MDS Analytical Technologies, Plaisir, France), in accordance with the manufacturer's protocol and as previously reported [43]. First-strand cDNA synthesis was carried out from total RNA using an oligo-dT primer and Super Script II reverse transcriptase (Invitrogen, Life Technologies). The mRNA amplifications were performed using the SYBR green Master Mix (Applied Biosystems). All reactions used a quantity of cDNA equivalent to 0.25 embryo, 0.3 μM of each primer, and an annealing temperature of 60°C. The primer sequences (Table 1) were obtained from the literature [44]. The expression of BCL2 and BAX mRNA was determined in each sample during independent assays. PCR reactions were set up in duplicate. The median value of PCR duplicates was considered and then expressed as the BCL-2/BAX ratio for each sample. The data are presented as means ± SD of three replicates.

TUNEL assay, active caspase-3 immunohistochemistry, and apotome microscopy

Nuclei with degraded DNA were detected by means of a technique based on the TUNEL principle [45] using fluorescein-conjugated dUTP, as described elsewhere with some minor modifications [17]. Three replicates of five to ten 8 dpf embryos per IVM/IVF treatment were permeabilized for 1 h in PBS with 0.5% (v/v) Triton X-100 (Sigma) and washed twice in PBS. As positive controls, some embryos were incubated in 50 units DNase/ml PBS (RQ1; Promega) for 30 min at 37°C and then washed twice in PBS. Embryos were incubated in 10 μl terminal deoxynucleotidyl transferase and 90 μl fluorescein-conjugated dUTP (TUNEL, In situ Cell Death Detection Kit, Roche) for 60 min in the dark. The embryos were washed once in 2X standard saline citrate buffer and then in PBS. The chromatin was stained with DAPI (diluted 1:1000 in PBS). In order to confirm the location of apoptotic activity assessed by TUNEL, five 8 dpf blastocysts per IVM/IVF treatment were submitted to the immunohistochemistry detection of active caspase-3, a downstream effector molecule in the DNA-degrading process, as described elsewhere with some minor modifications [16]. Briefly, permeabilized embryos were blocked in 0.01% PBS/triton X-100 (v/v) containing 2% (w/v) BSA for 1 h at 37°C, and then incubated overnight with a primary anti-active-caspase-3 antibody (D-175, polyclonal rabbit antibody; Cell Signaling Technology). After several washes, the embryos were incubated with a fluorescein isothiocyanate-conjugated antibody (711-165-152, donkey-anti-rabbit IgG antibody; Jackson ImmunoResearch; Interchim; see supplemntary antibody table). The primary and secondary antibodies were used at a dilution of 1:200. Omission of the primary antibody was used as negative control. The chromatin was then counterstained with DAPI (diluted 1:1000 in PBS). The embryos were mounted on slides with citifluor (Biovalley), and then observed using an inverted ZEISS AxioObserver Z1 microscope equipped with an ApoTome slider, a Colibri light source, and an Axiocam MRm camera controlled by Axiovision software (version 4.6) (MIMA2 imaging platform, INRA, Jouy-en-Josas, France). The total number of cells per embryo was estimated using ImageJ software (http://rsbweb.nih.gov/ij/), as routinely performed in our laboratory [33]. The method used to quantify TUNEL is summarized in Figure 2A. Series of images were acquired with optical sections in z every 2 μm for both the DAPI and TUNEL signals. Using ImageJ software (http://rsbweb.nih.gov/ij/), the area of the ICM was outlined manually on the image stack of the blastocyst, thus determining the region of interest (ROI) for each embryo. The ROI was then reproduced on each of the TUNEL and DAPI binary images of the ICM in order to determine the total integrative density for each signal. A constant arbitrary threshold value for each signal was used to create binary images. Finally, the total TUNEL fluorescence intensity was divided by the total DAPI signal to calculate normalized TUNEL levels. Three-dimensional (3D) projections of DAPI/TUNEL and DAPI/active caspase-3 labeling were reconstructed using IMARIS 8.3.1 software (Bitplane, Switzerland).

Statistical analysis

The Kolmogorov–Smirnov test was used to test the difference in the frequency distributions of the number of cells in 8 dpf blastocysts in relation to the IVM/IVF culture conditions. The distribution of 8 dpf blastocysts with more or less than 243 cells was then analyzed for the dose effects of PGE2 using a Kruskal–Wallis rank-sum test. Analysis of variance using general linear model was performed to test differences in embryo development, TUNEL signals, and the BCL-2/BAX mRNA expression ratio in relation to IVM/IVF culture conditions.

Table 2. In vitro development of bovine embryos derived from oocytes matured and fertilized in the presence of increasing doses of PGE2.

IVM/IVF Treatment	No. of oocytes		Embryo production*
PGE2 (μM)	Fertilized	Cleaved (%)	8 dpf blastocyst (%)
0	233	184 (78.9)	49 (26.6)
0.1	255	207 (81.2)	41 (19.8)
1	249	193 (77.5)	43 (22.3)
10	268	196 (73.1)	43 (21.9)

*Proportion of blastocysts relative to the total number of cleaved oocytes.

Differences in the numbers of day 15 conceptuses displaying or not a round, an elliptic epiblast, nonaxial, or axial were analyzed using the Fisher exact test. Differences in disk area and conceptus length were analyzed using the Mann–Whitney *U*-test. Significant differences were defined as $P < 0.05$. Analyses were performed using Systat 11 software (Systat Software).

Results

In vitro fertilization and blastocyst rates

As shown in Table 2, no differences in cleavage rates were evidenced when 0.1, 1, or 10 μM of PGE2 was added to the IVM/IVF culture media. In addition, the proportion of embryos developing until the blastocyst stage after the 8-day DIV culture period was similar in all treatment groups. No significant differences were found between the replicated experiments.

Cell numbers in blastocysts

A total of sixty-nine 8 dpf blastocysts were analyzed (15, 15, 24, and 15 for controls, 0.1, 1, and 10 μM PGE2 IVM/IVF treatment groups, respectively). Differences between the control and PGE2-treated IVM/IVF groups were found with respect to the number of cells in 8 dpf blastocysts. The number of blastomeres ranged from 113 to 243 (mean 179 $\pm$ 44) and from 80 to 430 (mean 212 $\pm$ 86) in embryos derived from the control and PGE2-treated (0.1, 1, and 10 μM PGE2 taken together) MIV/FIV groups, respectively. The PGE2 supplementation of IVM/IVF cultures significantly increased the proportion of derived 8 dpf blastocysts containing more than 243 blastomeres which was the maximum cell number assessed in the control group ($P < 0.05$; Figure 1A and B). The proportions of blastocysts containing more than 243 cells reached 46.7%, 33.3%, and 40% in embryo cultures derived from the IVM/IVF groups supplemented with 0.1, 1, and 10 μM PGE2, respectively. No dose-dependent effects were observed.

Apoptotic indices in blastocysts

The in situ detection of DNA fragmentation generated during the apoptotic process was performed using the TUNEL reaction. All sixty-nine 8 dpf blastocysts analyzed with fluorescent microscopy exhibited TUNEL. The ICM always displayed a TUNEL signal whereas TUNEL-labeled trophoblastic cells were only exceptionally observed (Figures 2B and 3A). The level of TUNEL signal quantified in the ICM was significantly reduced by the addition to IVM/IVF cultures of 0.1, 1, 10 μM PGE2, in a dose-dependent manner ($P < 0.05$; Figure 2C). No significant differences were found between the replicated experiments. The in situ detection of active caspase-3, a downstream

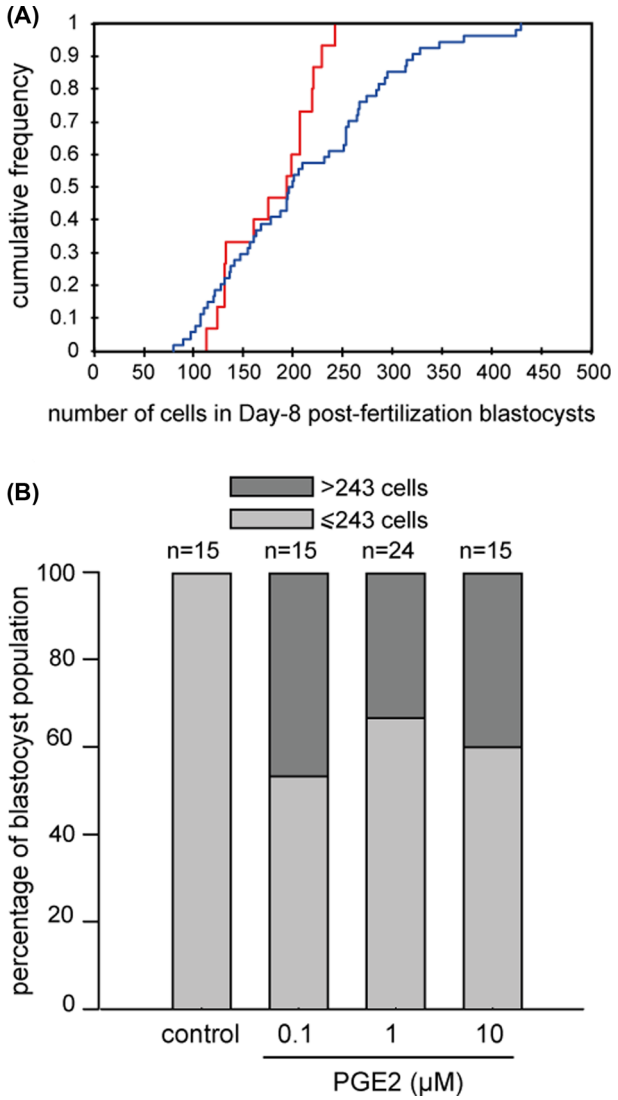

Figure 1. Assessment of total cell numbers in bovine day 8 postfertilization blastocysts. Cumulative frequency distribution of the number of cells in blastocysts derived from the control (red line) and PGE2-treated MIV/FIV (0.1, 1. 10 μM PGE2 all together, blue line) groups ($P < 0.05$) (**A**). Distribution of day 8 postfertilization blastocysts derived from IVM/IVF cultures supplemented with increasing doses of PGE2, 243 cells being the maximum blastomere number counted in control embryos ($P < 0.05$) (**B**).

effector molecule in the DNA-degrading process, was performed using an immunohistochemical procedure. As for the TUNEL signal, active caspase-3 staining was always displayed by the ICM whereas the trophoblast only displayed some sparse positive cells (Figure 3B). The transcript abundance of two selected apoptosis-related genes, anti-apoptotic factor BCL-2 and pro-apoptotic factor BAX, was also assessed. The inhibition of PTGS2 using 8 μM NS-398 during the IVM/IVF period significantly decreased the ratio of BCL-2/BAX mRNA expression in 8 dpf blastocysts ($P < 0.05$; Figure 4). The addition of 1 μM PGE2 to NS-398-treated IVM/IVF cultures restored a ratio that was comparable to that evaluated in the control group. The supplementation of IVM/IVF media with 1 μM PGE2 alone led to a ratio of BCL-2 to BAX mRNA expression that was significantly higher than that observed in embryos derived from the control group ($P < 0.05$; Figure 4). No significant differences were found between the replicated experiments.

Morphometry of day 15 conceptuses

In order to evaluate the in vivo development of blastocysts produced using different IVM/IVF treatments, seven sessions of 7 dpf blastocyst transfer into hormonally synchronized recipients were completed. A total of 78 day 15 conceptuses were recovered after flushing uterine horns 7 days later (30, 14, 20, and 14 among controls, with 8 μM NS-398 alone, with 8 μM NS-398+1 μM PGE2, and with 1 μM PGE2 alone in the IVM/IVF treatment groups, respectively). Among these, 62 conceptuses displayed intact ends (29, 10, 10, and 13 for controls, 8 μM NS-398 alone, 8 μM NS-398+1 μM PGE2, and 1 μM PGE2 alone in the IVM/IVF treatment groups, respectively) and 71 conceptuses displayed an embryonic disk (28, 12, 18, and 13 for controls, 8 μM NS-398 alone, 8 μM NS-398+1 μM PGE2, and 1 μM PGE2 alone IVM/IVF treatment groups, respectively). The IVM/IVF treatments led to a considerable disparity in the morphology of day 15 conceptuses regarding both the embryonic disk and extra-embryonic tissues (EET). The treatment of IVM/IVF cultures with 8 μM NS-398 significantly decreased the length of day 15 conceptuses ($P = 0.02$; Figure 5). The addition of 1 μM PGE2 to NS-398-treated cultures restored a median length similar to that measured in the control group ($P = 0.49$). Conceptus length increased significantly when 1 μM PGE2 alone was added to the IVM/IVF culture medium ($P = 0.001$). While the proportion of conceptuses with an embryonic disk was similar in all IVM/IVF treatment groups (93.3%, 85.8%, 90%, and 92.9%, respectively), marked differences in epiblast morphology were observed (Figure 6). Among the conceptuses generated under control IVM/IVF conditions, 64% displayed an elliptic epiblast. This proportion tended to decrease under PTGS2 inhibition using 8 μM NS-398 (33%, $P = 0.07$), whereas it reached a value comparable to that was observed under control conditions when NS-398-treated cultures were supplemented with 1 μM PGE2 (55%, $P = 0.76$). The addition of 1 μM PGE2 alone to MIV/FIV cultures led to 100% of retrieved conceptuses having an elliptic epiblast ($P = 0.01$). Moreover, all of them displayed an axial orientation, whereas the elliptic epiblasts of conceptuses derived from the other IVM/IVF treatment groups (control, 8 μM NS-398 supplemented or not with 1 μM PGE2) were shared between axial and nonaxial positioning. IVM/IVF treatment had no impact on the disk area associated with round or elliptic epiblast morphology (Figure 7). Overall, the disk area increased twofold during transition from a round to an elliptic shape ($P < 0.0001$; Figure 8).

Discussion

We had previously shown that PGE2 arising from upregulated PTGS2 activity in periconceptional CCs stimulates cell cycle progression during IVM and embryonic development up to blastulation in cattle [33]. The aim of the current study was to gain a further insight into the delayed effects of periconceptional PGE2 signaling on preimplantation embryonic development. We have now shown for the first time that the presence of PGE2 in the oocyte microenvironment exerts an inhibitory effect on the spontaneous cell death that occurs in embryonic cells at the blastocyst stage. Furthermore, our results indicate that this reduction in embryonic apoptosis is associated with more advanced stages of posthatching development at the levels of both the embryonic disk and EET 2 weeks after fertilization.

We had previously reported that the inhibition of cumulus PGE2 production by adding 8 μM NS-398 to MIV/FIV culture media slowed down the kinetics of initial embryonic cleavages and reduced

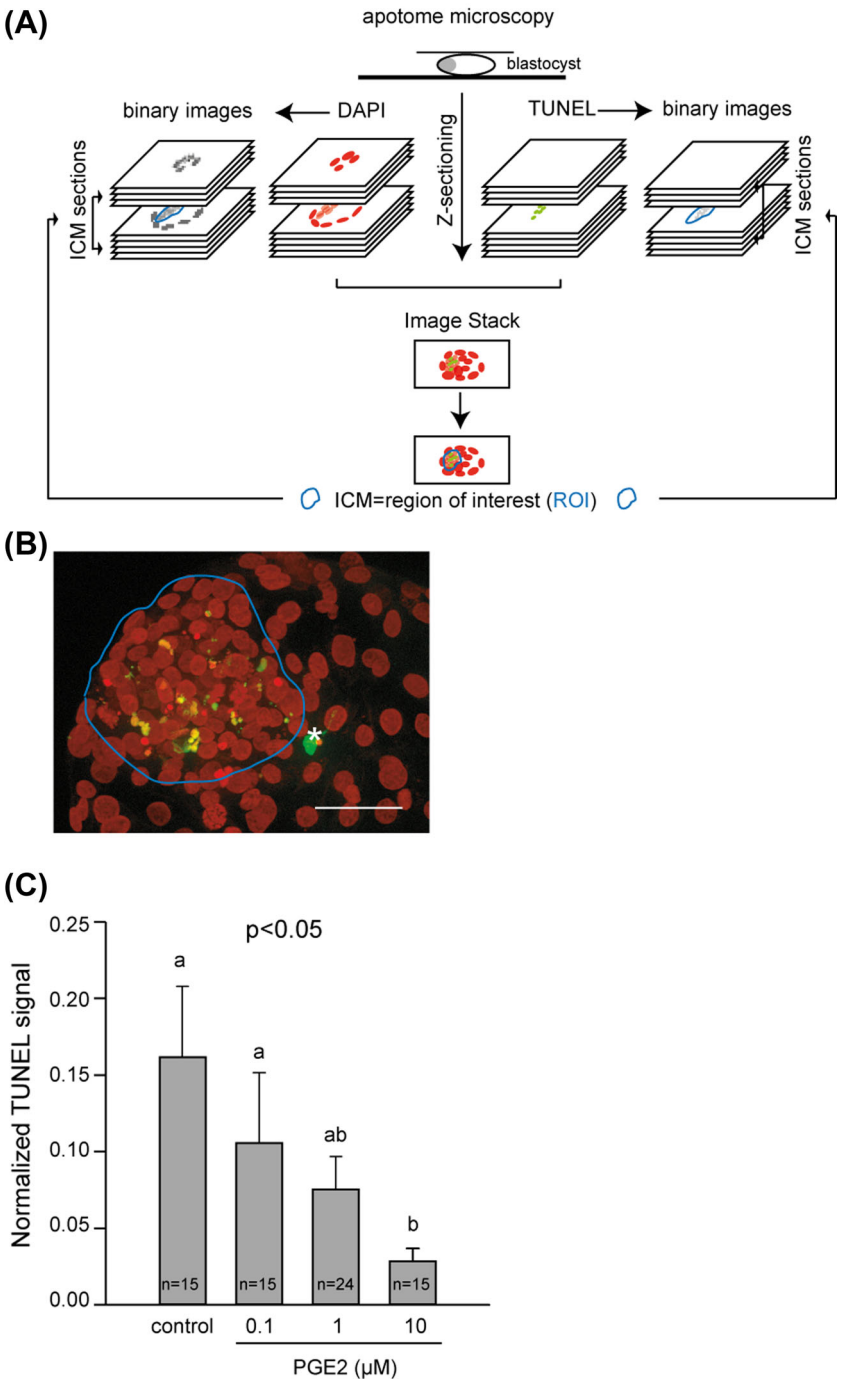

Figure 2. Quantification of TUNEL signals in the ICM of day 8 postfertilization bovine blastocysts derived from IVM/IVF cultures supplemented with increasing doses of PGE2. Schematic representation of the TUNEL quantification method (**A**). Photomicrograph shows a representative image stack of TUNEL (green) observed in a blastocyst (**B**). The ICM is outlined in blue. The chromatin is counterstained with DAPI (presented in red to contrast with the TUNEL). An asterisk (white) designates a TUNEL-positive trophoblastic cell (bar = 50 μm). Quantitative analysis of TUNEL signals detected in the ICM (**C**). Values are presented as the mean ± SEM of three independent experiments. Bars with different letters are significantly different *($P < 0.05$).*

overall blastomere numbers at the blastocyst stage in cattle [33]. In this study and using the same bovine model, we have shown that PGE2 supplementation during IVM and IVF led to a significant increase in total cell numbers per embryo from 0.1 μM PGE2, without changing the ability of derived zygotes in culture to reach the blastocyst stage at day 8 postfertilization. Overall, our data have clearly highlighted a relationship between the level of PGE2 present in the periconceptional microenvironment of the oocyte and the number of blastomeres present in the embryo at blastulation. As apoptosis represents a well-known physiological means of controlling embryonic cell populations, we examined whether periconceptional PGE2 could affect cell death that culminates in an embryo at the blastocyst

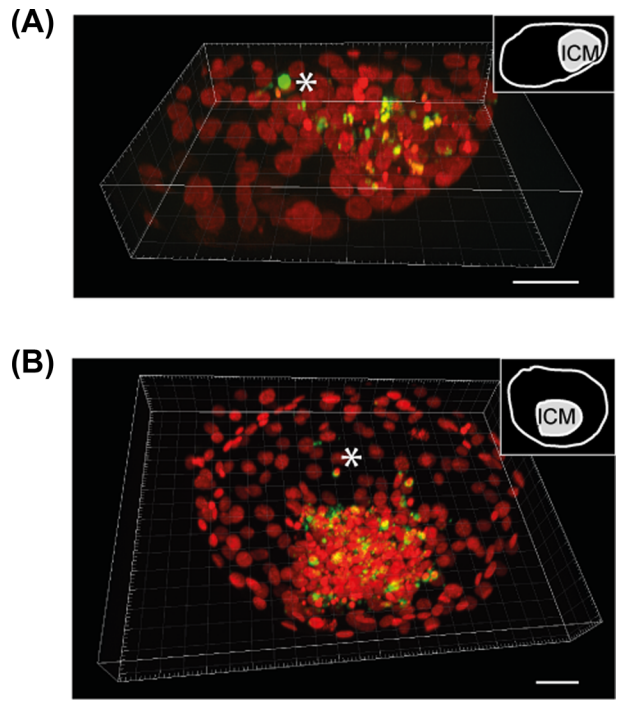

Figure 3. Three-dimensional reconstruction of TUNEL (**A**) and active caspase-3 (**B**) labeling (green) observed in day 8 postfertilization bovine blastocysts. The chromatin is counterstained with DAPI (presented in red to contrast with TUNEL and active caspase-3 labeling). Note that the both types of labeling are mainly located in the ICM of the blastocyst. An asterisk (white) designates a positive trophoblastic cell (bar = 50 μm).

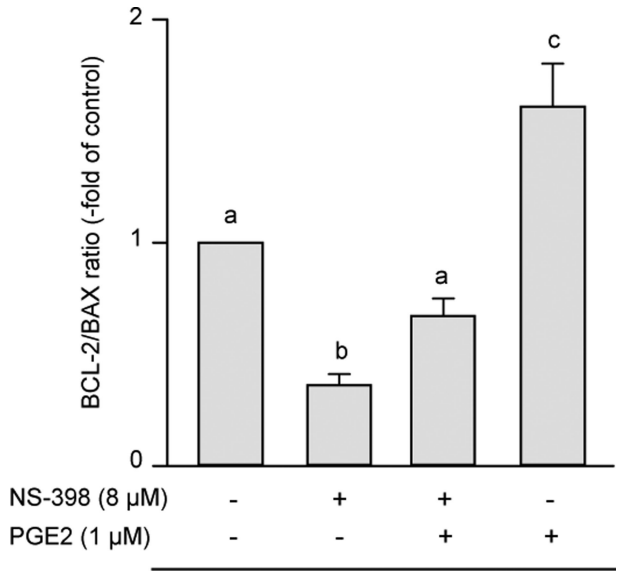

Figure 4. Quantitative analysis of the mRNA expression of apoptosis-related genes. Comparison of the BCL-2/BAX ratio in 8 dpf bovine blastocysts derived from IVM/IVF cultures supplemented or not with NS-398 and PGE2. Data are presented as the mean ± SD of three replicates. Bars with different letters depict significant statistical differences ($P < 0.05$).

stage during preimplantation development. Our results show that the highest levels of periconceptional PGE2 led to weaker apoptotic activities in blastocysts, as assessed by quantifying TUNEL signals and from the ratio of BCL-2 and BAX gene expression. Furthermore,

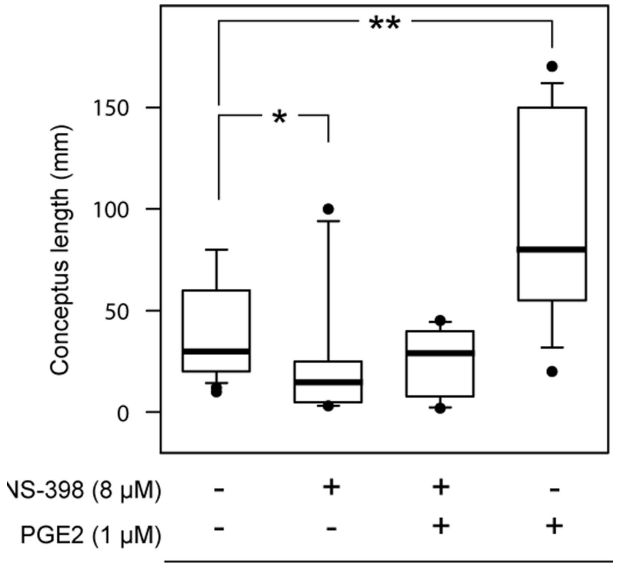

Figure 5. Length of bovine day 15 conceptuses derived from IVM/IVF cultures supplemented or not with NS-398 and PGE2. The box plots show median values (thick black bars), 25th and 75th percentiles (boxes), and 5th and 95th percentiles (whiskers). A significant difference is indicated by * ($P < 0.05$) and ** ($P < 0.0005$).

the significant increase in the incidence of embryonic apoptosis induced by periconceptional PTGS2 inhibition using 8 μM NS-398, and its return to a control level achieved by the 1 μM PGE2 supplementation of NS-398-treated IVM and IVF, provided evidence that cumulus PTGS2 activity promotes embryonic cell survival during preimplantation development, and this effect is mainly mediated by PGE2. Taken together, our previous and recent findings have both demonstrated that periconceptional PTGS2-related PGE2 is involved in the control of embryonic cell populations during early development via the regulation of cell cycle kinetics as well as apoptotic activity.

The ability of PTGS2-derived PGE2 to promote cell proliferation and survival is a hallmark of various cancers [35,36,46,47]. PGE2 is produced either in the tumor microenvironment or by the tumor cells themselves [35,48]. PGE2 exerts its effects at or near its site of secretion in an autocrine or paracrine manner, by activating specific receptors classified as PTGER1 to PTGER4. We have previously shown that bovine oocytes express PTGER2 and may be a direct target for the PGE2 produced by neighboring CCs [33]. Other prostaglandins related to PTGS2 activity may regulate cell proliferation and survival [49]. PGI2, released by trophoblastic cells during the peri-implantation period, has been shown to reduce apoptotic activity in mouse blastocyst [50]. However, the lasting effects of transient PGE2 impregnation in cell protecting from apoptosis have never previously been reported. Certain features of early embryonic development enabled us to refine the anti-apoptotic effect of PGE2. Gene expression does not occur during the first cleavage cycles in mammalian embryos. Early development is mainly dependent on maternal transcripts and proteins stored in the oocyte during oogenesis [51]. Embryonic transcription is gradually established while stores of maternal products diminish. In cattle, the EGA becomes effective as from the 8- to 16-cell stage [52]. Apoptotic cell death requires the de novo transcription of BAX and other proteins, rendering the preimplantation embryo refractory to spontaneous apoptotic activity before EGA [13,44]. On the other hand, the PGE2 is

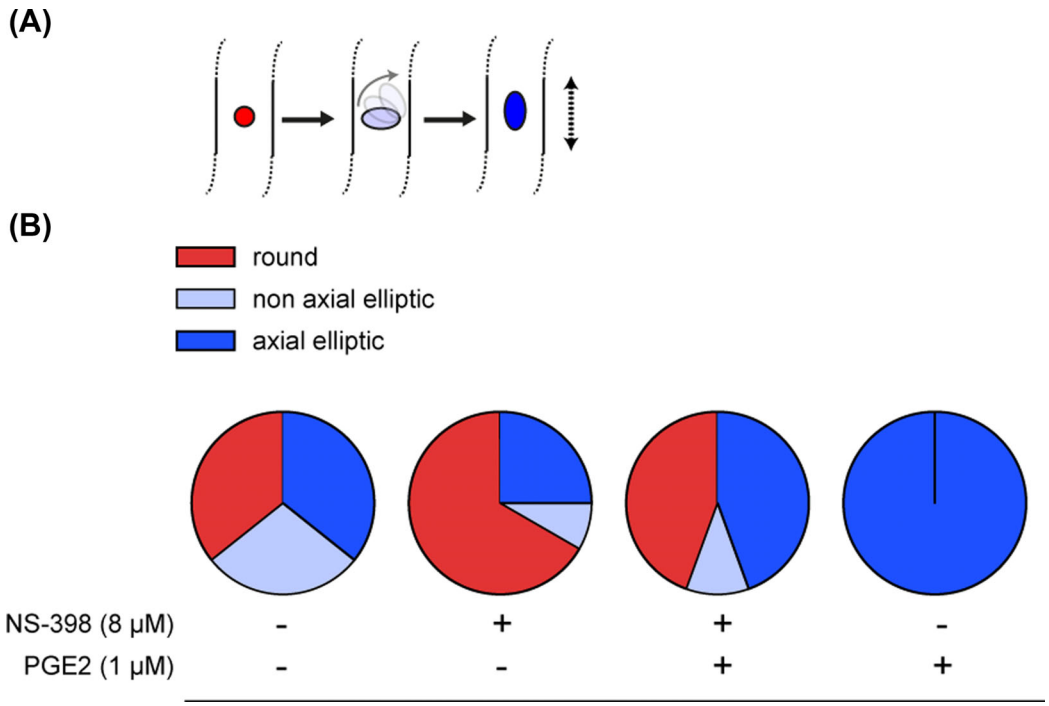

Figure 6. Embryonic disk morphology of bovine day 15 conceptuses derived from IVM/IVF cultures supplemented or not with NS-398 and PGE2. Type of embryonic disks according to their shape in the dorsal view categorized as round (red), nonaxial elliptic (light blue), and axial elliptic (deep blue) (**A**). The long axis of the elliptic epiblast gradually rotates (gray solid arrow) to become parallel to the elongation axis of the conceptus (black dotted arrow). Distribution of embryonic disks as a function of IVM/IVF culture conditions (**B**).

not stored but rapidly metabolized, as is the rule for locally acting lipid mediators [53]. Therefore, our investigations using an in vitro model of bovine embryo production provided evidence that transient PGE2 signaling can induce sustainable resistance to apoptosis throughout subsequent cell generations. A recent study using human endometriotic epithelial and stromal cell lines indicates that PGE2 can exert its biological effects through DNA methylation and histone modifications [54]. Further investigations will be necessary to determine whether underlying epigenetic mechanisms are involved in the lasting prosurvival action of PGE2 on bovine embryos.

As previously reported in other studies [11], our results of a TUNEL assay and active caspase-3 immunohistochemical staining showed that embryonic cell death was mainly located in the ICM at the blastocyst stage in cattle. In other species, such as pigs or humans, apoptotic cells are evenly distributed throughout the ICM and TE. However, the prognostic significance of the incidence of embryonic apoptosis on developmental potential remains undefined. It is generally acknowledged that cell death is a tightly regulated process that plays a major role in the control of cell populations throughout development [55]. Therefore, it is plausible to suppose that an altered apoptotic response induced in the embryo by inappropriate PGE2 signaling might impact posthatching development. Using key morphometric parameters that characterize posthatching development in cattle [56], we have now provided evidence that the level of PGE2 present in the periconceptional microenvironment of the oocyte strongly affects the developmental potential of both the ICM and TE compartments of the blastocyst. By means of grade-I day 7 postfertilization blastocyst transfer and day 15 conceptus collection procedures, we were able to observe that higher proportions of day 15 conceptuses with longer EET and an axial elliptic embryonic disk were recovered when the IVM/IVF culture conditions induced a lower incidence of apoptosis at the blastocyst stage. We further noted that the higher proportions of day 15 conceptuses with shorter EET length and a round embryonic disk were recovered when IVM/IVF cultures were performed under PTGS2 inhibition using 8 μM NS-398, or in other words IVM/IVF conditions inducing a higher incidence of embryonic apoptosis at the blastocyst stage. The restoration of posthatching development similar to that observed in the control group after 1 μM PGE2 supplementation of NS-398-treated IVM/IVF provided evidence that cumulus PTGS2 activity is involved in regulating the posthatching development of bovine embryos, and this effect is mainly mediated by PGE2. In ruminants, EET elongation results from rapid cell proliferation and gives rise to a large area of apposition with the endometrium that constitutes a critical requirement for the success of implantation [57]. Whether more extended EET at day 15 impacts the time of implantation and/or the outcome of pregnancy still needs to be explored. We and others have previously reported certain morphological features of the embryonic disk at the onset of gastrulation in ruminants [5–9]. Initially round, the dorsal shape of the embryonic disk becomes markedly elliptic as the conceptus becomes longer. Lengthening of the epiblast characterizes the onset of antero-posterior patterning of the embryo, leading to the formation of the primitive streak. The long axis of the elliptic epiblast, which is initially perpendicular to the elongation axis of the conceptus, gradually rotates to become parallel [58]. The epiblast gives rise to all future intraembryonic tissues and another extra-embryonic one, the mesoderm [59]. The underlying hypoblast is required for antero-posterior patterning of the epiblast-derived embryo proper [56]. During this study, we evidenced that the shift from a round to an elliptic dorsal shape was associated with a doubling of the embryonic disk area. Interestingly, we also noted that the area related to each type of embryonic disk

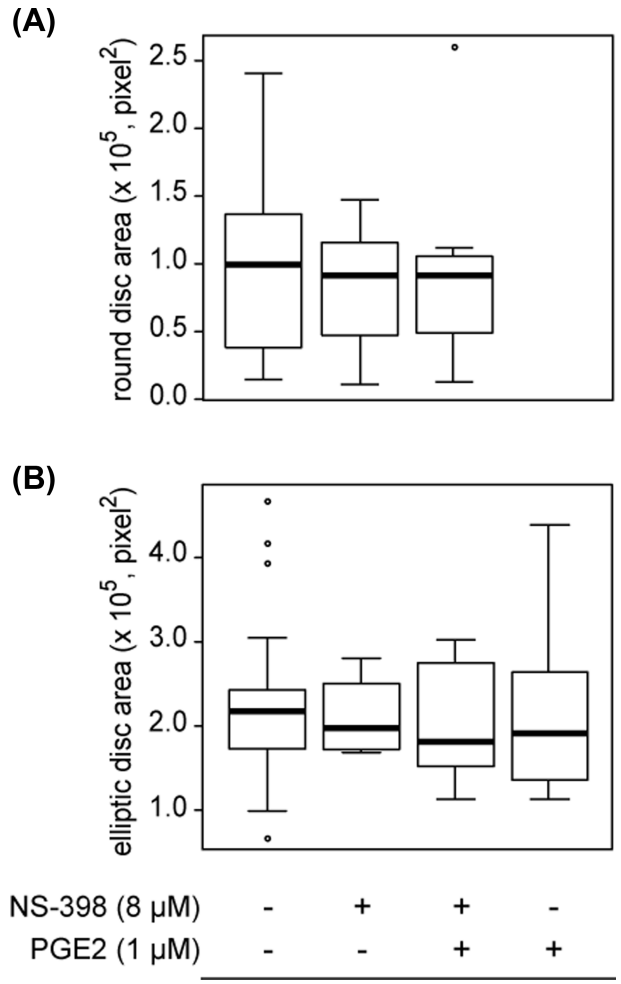

Figure 7. Quantification of disk area in bovine day 15 conceptuses derived from IVM/IVF cultures supplemented or not with NS-398 and PGE2. Epiblasts are classified according to the round (**A**) or elliptic (**B**) shape from a dorsal view and the IVM/IVF culture conditions. The box plots show median values (thick black bars), 25th and 75th percentiles (boxes), and 5th and 95th percentiles (whiskers). Note the absence of a significant difference between the IVM/IVF treatment groups.

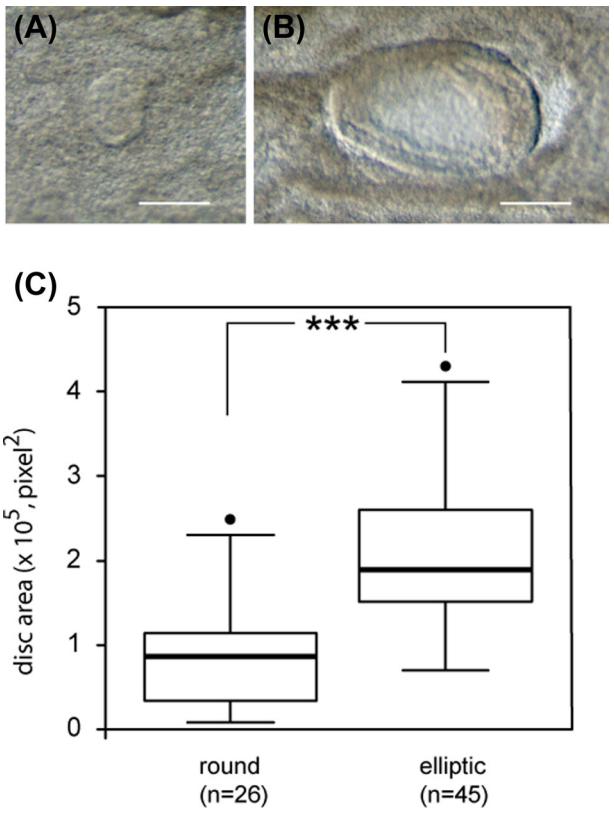

Figure 8. Quantification of disk area in all bovine conceptuses collected at day 15 after the transfer to recipients of in vitro produced day 7 blastocysts. Epiblasts are divided into round (**A**) or elliptic shape from a dorsal view (**B**) (bar = 200 μm). The box plots show median values (thick black bars), 25th and 75th percentiles (boxes), and 5th and 95th percentiles (whiskers) (**C**). A significant difference is indicated by *** ($P < 0.0001$).

morphology remained unaffected by the level of periconceptional PGE2. This finding suggests that the initiation of antero-posterior patterning occurs when a threshold cell population size is reached by the embryonic disk, as shown previously in the mouse embryo [60]. Taken together, our present findings provide evidence that periconceptional PTGS2-derived PGE2 is involved in controlling the cell population of the preimplantation conceptus, linking the incidence of embryonic apoptosis to the timing of the establishment of antero-posterior polarity and the extent of the elongation process during posthatching development.

To summarize, our previous and present studies have accumulated evidence of a critical physiological role for periconceptional PTGS2-related PGE2 in regulating cell survival and proliferation of the first lineages during preimplantation development. PTGS2-related PGE2 produced by the somatic compartment of the pre-ovulatory follicle some hours before ovulation could represent a key player in the mechanisms that can drive successful early development until the moment of implantation.

Supplementary data

Supplementary data are available at *BIOLRE* online.

Acknowledgment

The authors gratefully acknowledge the assistance provided by the technical team at the INRA experimental station of Bressonvilliers (UCEA). The authors also like to thank V. Gelin and, A. Neveux for their help during this study.

References

1. Artus J, Chazaud C. A close look at the mammalian blastocyst: epiblast and primitive endoderm formation. *Cell Mol Life Sci* 2014; **71**:3327–3338.
2. De Paepe C, Krivega M, Cauffman G, Geens M, Van de Velde H. Totipotency and lineage segregation in the human embryo. *Mol Hum Reprod* 2014; **20**:599–618.
3. Sheng G. Epiblast morphogenesis before gastrulation. *Dev Biol* 2015; **401**:17–24.
4. Degrelle SA, Campion E, Cabau C, Piumi F, Reinaud P, Richard C, Renard JP, Hue I. Molecular evidence for a critical period in mural trophoblast development in bovine blastocysts. *Dev Biol* 2005; **288**:448–460.
5. Degrelle SA, Le Cao KA, Heyman Y, Everts RE, Campion E, Richard C, Ducroix-Crepy C, Tian XC, Lewin HA, Renard JP, Robert-Granie C, Hue I. A small set of extra-embryonic genes defines a new landmark for bovine embryo staging. *Reproduction* 2011; **141**:79–89.

6. Blomberg L, Hashizume K, Viebahn C. Blastocyst elongation, trophoblastic differentiation, and embryonic pattern formation. *Reproduction* 2008; **135**:181–195.
7. Hue I, Degrelle SA, Campion E, Renard JP. Gene expression in elongating and gastrulating embryos from ruminants. *Soc Reprod Fertil Suppl* 2007; **64**:365–377.
8. Guillomot M, Turbe A, Hue I, Renard JP. Staging of ovine embryos and expression of the T-box genes Brachyury and Eomesodermin around gastrulation. *Reproduction* 2004; **127**:491–501.
9. Maddox-Hyttel P, Alexopoulos NI, Vajta G, Lewis I, Rogers P, Cann L, Callesen H, Tveden-Nyborg P, Trounson A. Immunohistochemical and ultrastructural characterization of the initial post-hatching development of bovine embryos. *Reproduction* 2003; **125**:607–623.
10. Hardy K. Cell death in the mammalian blastocyst. *Mol Hum Reprod* 1997; **3**:919–925.
11. Fabian D, Koppel J, Maddox-Hyttel P. Apoptotic processes during mammalian preimplantation development. *Theriogenology* 2005; **64**:221–231.
12. Hansen PJ, Fear JM. Cheating death at the dawn of life: developmental control of apoptotic repression in the preimplantation embryo. *Biochem Biophys Res Commun* 2011; **413**:155–158.
13. Gjorret JO, Knijn HM, Dieleman SJ, Avery B, Larsson LI, Maddox-Hyttel P. Chronology of apoptosis in bovine embryos produced in vivo and in vitro. *Biol Reprod* 2003; **69**:1193–1200.
14. Pomar FJ, Teerds KJ, Kidson A, Colenbrander B, Tharasanit T, Aguilar B, Roelen BA. Differences in the incidence of apoptosis between in vivo and in vitro produced blastocysts of farm animal species: a comparative study. *Theriogenology* 2005; **63**:2254–2268.
15. Leidenfrost S, Boelhauve M, Reichenbach M, Gungor T, Reichenbach HD, Sinowatz F, Wolf E, Habermann FA. Cell arrest and cell death in mammalian preimplantation development: lessons from the bovine model. *PLoS One* 2011; **6**:e22121.
16. Gjorret JO, Fabian D, Avery B, Maddox-Hyttel P. Active caspase-3 and ultrastructural evidence of apoptosis in spontaneous and induced cell death in bovine in vitro produced pre-implantation embryos. *Mol Reprod Dev* 2007; **74**:961–971.
17. Knijn HM, Gjorret JO, Vos PL, Hendriksen PJ, van der Weijden BC, Maddox-Hyttel P, Dieleman SJ. Consequences of in vivo development and subsequent culture on apoptosis, cell number, and blastocyst formation in bovine embryos. *Biol Reprod* 2003; **69**:1371–1378.
18. Van Hoeck V, Bols PE, Binelli M, Leroy JL. Reduced oocyte and embryo quality in response to elevated non-esterified fatty acid concentrations: a possible pathway to subfertility? *Anim Reprod Sci* 2014; **149**:19–29.
19. Kleijkers SH, Eijssen LM, Coonen E, Derhaag JG, Mantikou E, Jonker MJ, Mastenbroek S, Repping S, Evers JL, Dumoulin JC, van Montfoort AP. Differences in gene expression profiles between human preimplantation embryos cultured in two different IVF culture mediadagger. *Hum Reprod* 2015; **30**:2303–2311.
20. Pomini Pinto RF, Fontes PK, Loureiro B, Sousa Castilho AC, Sousa Ticianelli J, Montanari Razza E, Satrapa RA, Buratini J, Moraes Barros C. Effects of FGF10 on bovine oocyte meiosis progression, apoptosis, embryo development and relative abundance of developmentally important genes in vitro. *Reprod Domest Anim* 2015; **50**:84–90.
21. Diskin MG, Parr MH, Morris DG. Embryo death in cattle: an update. *Reprod Fertil Dev* 2011; **24**:244–251.
22. Lonergan P, Fair T, Forde N, Rizos D. Embryo development in dairy cattle. *Theriogenology* 2016; **86**:270–277.
23. Wiltbank MC, Baez GM, Garcia-Guerra A, Toledo MZ, Monteiro PL, Melo LF, Ochoa JC, Santos JE, Sartori R. Pivotal periods for pregnancy loss during the first trimester of gestation in lactating dairy cows. *Theriogenology* 2016; **86**:239–253.
24. Assidi M, Montag M, Sirard MA. Use of both cumulus cells' transcriptomic markers and zona pellucida birefringence to select developmentally competent oocytes in human assisted reproductive technologies. *BMC Genomics* 2015; **16** (suppl 1):S9.
25. Khan DR, Landry DA, Fournier E, Vigneault C, Blondin P, Sirard MA. Transcriptome meta-analysis of three follicular compartments and its correlation with ovarian follicle maturity and oocyte developmental competence in cows. *Physiol Genomics* 2016; **48**:633–643.
26. McKenzie LJ, Pangas SA, Carson SA, Kovanci E, Cisneros P, Buster JE, Amato P, Matzuk MM. Human cumulus granulosa cell gene expression: a predictor of fertilization and embryo selection in women undergoing IVF. *Hum Reprod* 2004; **19**:2869–2874.
27. Nuttinck F, Reinaud P, Tricoire H, Vigneron C, Peynot N, Mialot JP, Mermillod P, Charpigny G. Cyclooxygenase-2 is expressed by cumulus cells during oocyte maturation in cattle. *Mol Reprod Dev* 2002; **61**:93–101.
28. Takahashi T, Morrow JD, Wang H, Dey SK. Cyclooxygenase-2-derived prostaglandin E(2) directs oocyte maturation by differentially influencing multiple signaling pathways. *J Biol Chem* 2006; **281**:37117–37129.
29. Duffy DM. Novel contraceptive targets to inhibit ovulation: the prostaglandin E2 pathway. *Hum Reprod Update* 2015; **21**:652–670.
30. Liu J, Carriere PD, Dore M, Sirois J. Prostaglandin G/H synthase-2 is expressed in bovine preovulatory follicles after the endogenous surge of luteinizing hormone. *Biol Reprod* 1997; **57**:1524–1531.
31. Nuttinck F, Marquant-Le Guienne B, Clement L, Reinaud P, Charpigny G, Grimard B. Expression of genes involved in prostaglandin E2 and progesterone production in bovine cumulus-oocyte complexes during in vitro maturation and fertilization. *Reproduction* 2008; **135**:593–603.
32. Sugimoto Y, Narumiya S. Prostaglandin E receptors. *J Biol Chem* 2007; **282**:11613–11617.
33. Nuttinck F, Gall L, Ruffini S, Laffont L, Clement L, Reinaud P, Adenot P, Grimard B, Charpigny G, Marquant-Le Guienne B. PTGS2-related PGE2 affects oocyte MAPK phosphorylation and meiosis progression in cattle: late effects on early embryonic development. *Biol Reprod* 2011; **84**:1248–1257.
34. Hizaki H, Segi E, Sugimoto Y, Hirose M, Saji T, Ushikubi F, Matsuoka T, Noda Y, Tanaka T, Yoshida N, Narumiya S, Ichikawa A. Abortive expansion of the cumulus and impaired fertility in mice lacking the prostaglandin E receptor subtype EP(2). *Proc Natl Acad Sci USA* 1999; **96**:10501–10506.
35. Abrahao AC, Castilho RM, Squarize CH, Molinolo AA, dos Santos-Pinto D, Jr, Gutkind JS. A role for COX2-derived PGE2 and PGE2-receptor subtypes in head and neck squamous carcinoma cell proliferation. *Oral Oncol* 2010; **46**:880–887.
36. Wang D, Dubois RN. Eicosanoids and cancer. *Nat Rev Cancer* 2010; **10**:181–193.
37. Richard C, Hue I, Gelin V, Neveux A, Campion E, Degrelle SA, Heyman Y, Chavatte-Palmer P. Transcervical collection of bovine embryos up to Day 21: an 8-year overview. *Theriogenology* 2015; **83**:1101–1109.
38. Degrelle SA, Jaffrezic F, Campion E, Le Cao KA, Le Bourhis D, Richard C, Rodde N, Fleurot R, Everts RE, Lecardonnel J, Heyman Y, Vignon X et al. Uncoupled embryonic and extra-embryonic tissues compromise blastocyst development after somatic cell nuclear transfer. *PLoS One* 2012; **7**:e38309.
39. Mansouri-Attia N, Sandra O, Aubert J, Degrelle S, Everts RE, Giraud-Delville C, Heyman Y, Galio L, Hue I, Yang X, Tian XC, Lewin HA et al. Endometrium as an early sensor of in vitro embryo manipulation technologies. *Proc Natl Acad Sci USA* 2009; **106**:5687–5692.
40. Hady PJ, Domecq JJ, Kaneene JB. Frequency and precision of body condition scoring in dairy cattle. *J Dairy Sci* 1994; **77**:1543–1547.
41. Parrish JJ, Susko-Parrish J, Winer MA, First NL. Capacitation of bovine sperm by heparin. *Biol Reprod* 1988; **38**:1171–1180.
42. Holm P, Booth PJ, Schmidt MH, Greve T, Callesen H. High bovine blastocyst development in a static in vitro production system using SOFaa medium supplemented with sodium citrate and myo-inositol with or without serum-proteins. *Theriogenology* 1999; **52**:683–700.
43. Khan DR, Dube D, Gall L, Peynot N, Ruffini S, Laffont L, Le Bourhis D, Degrelle S, Jouneau A, Duranthon V. Expression of pluripotency master regulators during two key developmental transitions: EGA and early lineage specification in the bovine embryo. *PLoS One* 2012; **7**:e34110.
44. Fear JM, Hansen PJ. Developmental changes in expression of genes involved in regulation of apoptosis in the bovine preimplantation embryo. *Biol Reprod* 2011; **84**:43–51.
45. Gavrieli Y, Sherman Y, Ben-Sasson SA. Identification of programmed cell death in situ via specific labeling of nuclear DNA fragmentation. *J Cell Biol* 1992; **119**:493–501.

46. Castellone MD, Teramoto H, Gutkind JS. Cyclooxygenase-2 and colorectal cancer chemoprevention: the beta-catenin connection. *Cancer Res* 2006; **66**:11085–11088.
47. Greenhough A, Wallam CA, Hicks DJ, Moorghen M, Williams AC, Paraskeva C. The proapoptotic BH3-only protein Bim is downregulated in a subset of colorectal cancers and is repressed by antiapoptotic COX-2/PGE(2) signalling in colorectal adenoma cells. *Oncogene* 2010; **29**:3398–3410.
48. Rasmuson A, Kock A, Fuskevag OM, Kruspig B, Simon-Santamaria J, Gogvadze V, Johnsen JI, Kogner P, Sveinbjornsson B. Autocrine prostaglandin E2 signaling promotes tumor cell survival and proliferation in childhood neuroblastoma. *PLoS One* 2012; **7**:e29331.
49. Yagami T, Koma H, Yamamoto Y. Pathophysiological roles of cyclooxygenases and prostaglandins in the central nervous system. *Mol Neurobiol* 2016; **53**:4754–4771.
50. Pakrasi PL, Jain AK. Cyclooxygenase-2-derived endogenous prostacyclin reduces apoptosis and enhances embryo viability in mouse. *Prostaglandins Leukot Essent Fatty Acids* 2008; **79**:27–33.
51. Deutsch DR, Frohlich T, Otte KA, Beck A, Habermann FA, Wolf E, Arnold GJ. Stage-specific proteome signatures in early bovine embryo development. *J Proteome Res* 2014; **13**:4363–4376.
52. Graf A, Krebs S, Heininen-Brown M, Zakhartchenko V, Blum H, Wolf E. Genome activation in bovine embryos: review of the literature and new insights from RNA sequencing experiments. *Anim Reprod Sci* 2014; **149**:46–58.
53. Legler DF, Bruckner M, Uetz-von Allmen E, Krause P. Prostaglandin E2 at new glance: novel insights in functional diversity offer therapeutic chances. *Int J Biochem Cell Biol* 2010; **42**:198–201.
54. Arosh JA, Lee J, Starzinski-Powitz A, Banu SK. Selective inhibition of prostaglandin E2 receptors EP2 and EP4 modulates DNA methylation and histone modification machinery proteins in human endometriotic cells. *Mol Cell Endocrinol* 2015; **409**:51–58.
55. Zakeri Z, Penaloza CG, Smith K, Ye Y, Lockshin RA. What cell death does in development. *Int J Dev Biol* 2015; **59**:11–22.
56. van Leeuwen J, Berg DK, Pfeffer PL. Morphological and gene expression changes in cattle embryos from hatched blastocyst to early gastrulation stages after transfer of in vitro produced embryos. *PLoS One* 2015; **10**:e0129787.
57. Ribeiro ES, Greco LF, Bisinotto RS, Lima FS, Thatcher WW, Santos JE. Biology of preimplantation conceptus at the onset of elongation in dairy cows. *Biol Reprod* 2016; **94**:97.
58. Eakin GS, Behringer RR. Diversity of germ layer and axis formation among mammals. *Semin Cell Dev Biol* 2004; **15**:619–629.
59. Schroder SS, Tsikolia N, Weizbauer A, Hue I, Viebahn C. Paraxial nodal expression reveals a novel conserved structure of the left-right organizer in four mammalian species. *Cells Tissues Organs* 2016; **201**: 77–87.
60. Lewis NE, Rossant J. Mechanism of size regulation in mouse embryo aggregates. *J Embryol Exp Morphol* 1982; **72**:169–181.